


Small scale structures of turbulence in terms of entropy and fluctuation theorems

André Fuchs ^{1,*} Sílvio M. Duarte Queirós,² Pedro G. Lind,^{3,4} Alain Girard,⁵ Freddy Bouchet,⁶ Matthias Wächter,¹ and Joachim Peinke¹

¹*Institute of Physics and ForWind, University of Oldenburg, Küppersweg 70, D-26129 Oldenburg, Germany*

²*Centro Brasileiro de Pesquisas Físicas and National Institute of Science and Technology for Complex Systems, Rua Dr. Xavier Sigaud 150, 2290-180 Urca, Rio de Janeiro–RJ, Brazil*

³*Department of Computer Science, OsloMet–Oslo Metropolitan University, 4 St. Olavs plass, N-0130 Oslo, Norway*

⁴*Instituto Universitário de Lisboa (ISCTE-IUL), ISTAR-IUL, Avenida Forças Armadas, P-1649-026 Lisboa, Portugal*

⁵*INAC-SBT, UMR CEA-Grenoble University, CEA Grenoble, 17 rue des Martyrs, F-38054 Grenoble, France*

⁶*Univ Lyon, Ens de Lyon, Univ Claude Bernard, CNRS, Laboratoire de Physique, F-69364 Lyon, France*



(Received 5 April 2019; accepted 29 January 2020; published 11 March 2020)

We present experimental evidence that, together with the integral fluctuation theorem, which is fulfilled with high accuracy, a detailed-like fluctuation theorem holds for large entropy values in cascade processes in turbulent flows. Based on experimental data, we estimate the stochastic equations describing the scale-dependent cascade process in a turbulent flow by means of Fokker-Planck equations, and from the corresponding individual cascade trajectories an entropy term can be determined. Since the statistical fluctuation theorems set the occurrence of positive and negative entropy events in strict relation, we are able to verify how cascade trajectories, defined by entropy consumption or entropy production, are linked to turbulent structures: Trajectories with entropy production start from large velocity increments at large scale and converge to zero velocity increments at small scales; trajectories with entropy consumption end at small scale velocity increments with finite size and show a lower bound for small scale increments. A linear increase with the magnitude of the negative entropy value is found. This indicates a tendency to local discontinuities in the velocity field. Our findings show no lower bound of negative entropy values and thus for the corresponding piling up velocity differences of the small scale structures.

DOI: [10.1103/PhysRevFluids.5.034602](https://doi.org/10.1103/PhysRevFluids.5.034602)

I. INTRODUCTION

One fundamental task in turbulence is to understand it as the result of a cascade process through a hierarchy of spatial and temporal scales. There have been breakthroughs to achieve this task, such as the derivation of the Kármán-Howarth equation and Kolmogorov's four-fifths law [1–3]. Despite the progress made, a basic problem of understanding the small scale structure of turbulence is still missing, as expressed mathematically as one Millennium problem [4] or by the discussion of blowup or singularities (for some recent works, see Refs. [5–7]). In Ref. [2] singularities and depletions are named as two central problems of turbulence for which rigorous methods should be found.

*andre.fuchs@uni-oldenburg.de

Besides the aforementioned approaches, turbulence has also been described by means of a cascade trajectory which assumes a stochastic process with respect to the evolution process of velocity increments from large scales towards smaller scales. The bridge between theory and experiments is made by assuming parameter-free methods for deriving an empirical Fokker-Planck equation for the cascade process, which incorporates the multiscale statistics of velocity increments [8–13].

Thermodynamically, we can understand turbulence, especially the cascade trajectory, as a process leading a fluid under specific conditions (Reynolds number) from a nonequilibrium state into a new nonequilibrium state by the combination of energy injection and dissipation. Within this context, the stochastic approach to turbulence has recently been linked to stochastic thermodynamics [12,14], also called stochastic energetics [15], developed previously in Refs. [16–19]. Actually, experimental studies of stochastic thermodynamics mainly focus on particle systems, such as biological and nanosystems [20,21], which are assumed to be well off the thermodynamic limit so that the probabilistic nature of thermodynamic relations becomes clearer.

Herein, we present a step forward by showing how fundamental results in nonequilibrium thermodynamics are associated with typical features observed in turbulent flows, which is a classical continuous macroscopic system without atomic or molecular features. A basic aspect is that the stochastic thermodynamics enables one to define a total entropy variation for each cascade trajectory. For this total entropy variation, we show that the integral fluctuation theorem is fulfilled with high accuracy, proposing this as another fundamental law for turbulence and showing the consistency of the empirical Fokker-Planck description. Positive and negative total entropy variations, respectively consumptions, are furthermore balanced in a certain range by an extended or detailed-like fluctuation theorem. We show that the estimation of entropies allows us to select a distinct realization of a turbulent cascade trajectory leading to interesting small scale structures, such as piling up fluctuations and finite “jumps” for entropy-consuming trajectories.

II. EXPERIMENTAL SETUP

In this paper, we report on an analysis of a turbulent flow generated by a fractal grid placed at the inlet of the test section in a closed loop wind tunnel. The results presented here do not depend on the specific selection of this turbulence experiment. Similar results were found for other turbulent flows such as a free jet. The experimental setup is sketched in Fig. 1(a). Constant temperature hot-wire anemometry measurements of velocity were done at a distance of 54 cm along the centerline. To account for the distance at which the different wakes generated by the fractal grid bars interact, Mazellier and Vassilicos introduced [22] the wake-interaction length scale x_* ($54 \text{ cm} \hat{=} 0.6x_*$). The data acquisition comprises 6.4×10^7 samples at a sampling frequency of 60 kHz. The inlet velocity was set to $\langle v \rangle = 15.3 \text{ m/s}$. The turbulent flow is characterized by an integral length of $L = 28 \text{ mm}$ and a Taylor length scale of $\lambda = 2.5 \text{ mm}$, corresponding to $\text{Re}_L = u' L / \nu = 4540$ and $\text{Re}_\lambda = u' \lambda / \nu = 405$, respectively, where u' is the root mean square of velocity fluctuations related to the mean value and ν is the kinematic viscosity.

III. METHODS OF ANALYSIS

From a data series of velocities $v(t)$ (a component in the direction of the mean flow) we construct the data sets of their longitudinal increments $u_\tau(t) = v(t) - v(t + \tau)$ labeled by the timescale τ which, assuming the Taylor hypothesis [23] (the turbulence intensity is less than 20% for the analyzed data), corresponds to spatial velocity increments, $u_r(t) = -u_\tau(t)$ with $r = -\tau \langle v \rangle$.

Based on increments we define cascade trajectories $[u(\cdot)] = \{u_L, \dots, u_\lambda\}$ for different scales from the integral length L to the Taylor length λ scale. We assume that a single trajectory represents one realization of the turbulent cascade process and a large number of these trajectories reflect the statistics caused by the process. An illustration of one cascade trajectory or a single “cascade path” is plotted in Fig. 1(b). As shown in this figure, we use the following normalization to compare the results of different data sets. The scale r is given in units of Taylor length scale λ and the velocity

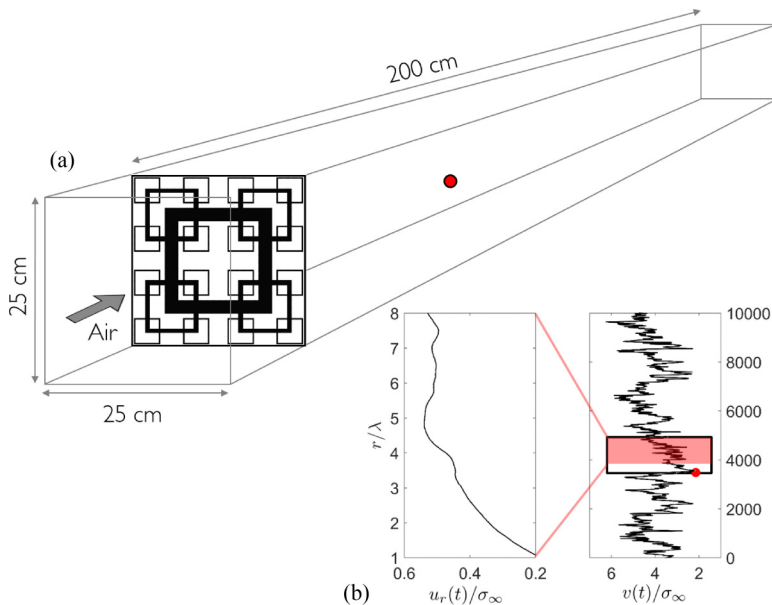


FIG. 1. (a) Illustration of experimental setup. The fractal grid is placed at the inlet of the test section in a closed loop wind tunnel. The red dot marks the position of hot-wire measurement. (b) Exemplification of a single cascade trajectory $[u(\cdot)]$, obtained by splitting the velocity time series $v(t)$ (right) into intervals of integral length scales and calculating the velocity increments with respect to the point at the beginning of these intervals.

increments u_r are given in units of the standard deviation at infinite scales $\sigma_\infty = \sqrt{2}\sigma_v = 3.5$ m/s [σ_v is the standard deviation of the velocity time series $v(t)$].

Next, we show how the stochastic evolution of cascade trajectories can be described by a Fokker-Planck equation in scale [9,11,24],

$$-\partial_r p(u_r|u_{r_0}) = -\partial_{u_r} [D^{(1)}(u_r, r)p(u_r|u_{r_0})] + \partial_{u_r}^2 [D^{(2)}(u_r, r)p(u_r|u_{r_0})], \quad (1)$$

with $r < r_0$. We use the abbreviations $u_r = u_r(t)$, $\partial_r = \partial/\partial r$, and $\partial_u = \partial/\partial u_r$. The negative sign on the left-hand side of Eq. (1) is due to the direction of the cascade process from large to small scales r . Experimental evidence shows that the Markov property can be assumed to hold for the cascade coarse-grained by the Einstein-Markov length $\Delta_{EM} \approx 0.9\lambda$ [24,25]. The coarsening means that it does not make any sense to investigate increment structures on smaller scales than Δ_{EM} or respectively λ by the presented method. That is the reason why the definition of the cascade trajectories ends at λ . Consequently, all information in the cascade trajectories can be derived from three-point (two-scale) statistics (see Ref. [13] for further details).

The two functions $D^{(1,2)}$ defining the Fokker-Planck equation are called drift and diffusion coefficients, respectively, and are defined by the two first conditional moments ($k = 1, 2$), known as Kramers-Moyal coefficients,

$$D^{(k)}(u_r, r) = \lim_{r' \rightarrow r} \frac{\int_{-\infty}^{\infty} (u_{r'} - u_r)^k p(u_{r'}|u_r) du_{r'}}{k!(r' - r)}. \quad (2)$$

$D^{(k)}$ can be estimated directly from measured data by an optimization procedure proposed in Refs. [8,10,12], which includes reconstruction of the conditional probability density functions $p(u_{r'}|u_r)$ via a short time propagator [26]. Note, there are different definitions of $D^{(k)}$ with respect to a multiplication with r (see Ref. [13]).

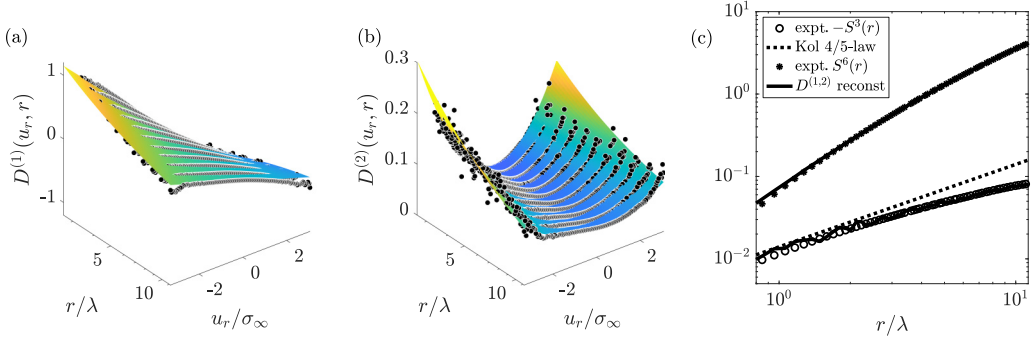


FIG. 2. (a) First- and (b) second-order Kramers-Moyal coefficients estimated from experimental data. Linear and parabolic fitting functions [Eqs. (3) and (4)] illustrate their functional dependency. (c) Third- and sixth-order structure functions as a function of the scale. Shown are the experimental data (expt.) and the reconstruction using the fitted Kramers-Moyal coefficients. We plot $-S^3(r)$ since the third-order structure function is negative in the inertial range. The dashed line represents the four-fifths law, that is expected to hold only for ideal flow conditions (homogeneous isotropic turbulence) and for a very large or infinitely large Reynolds number. The sixth-order structure function allows one to determine Kolmogorov's intermittency correction $S^6(r) \propto r^{2-\mu}$.

Similarly to previous works [10–12,24], here we find a linear function for $D^{(1)}$ and a parabolic function for $D^{(2)}$,

$$D^{(1)}(u_r, r) = d_{11}(r)u_r, \quad (3)$$

$$D^{(2)}(u_r, r) = d_{22}(r)u_r^2 + d_{21}(r)u_r + d_{20}(r). \quad (4)$$

The estimated drift and diffusion coefficients and the fits defined in Eqs. (3) and (4) are plotted in Figs. 2(a) and 2(b). Coefficients d_{ij} in the fits are functions of scale r of the form $\alpha(r/\lambda)^\beta + \gamma$,

$$d_{11}(r) = -0.73(r/\lambda)^{-0.61} + 0.05,$$

$$d_{22}(r) = 0.05(r/\lambda)^{-0.68} - 0.01,$$

$$d_{21}(r) = -0.04(r/\lambda)^{-0.29} + 0.02,$$

$$d_{20}(r) = 0.79(r/\lambda)^{0.01} - 0.76.$$

In the spirit of nonequilibrium stochastic thermodynamics [27] it is possible to associate with every individual cascade trajectory $[u(\cdot)]$ (obtained by the definition given above) a total entropy variation ΔS_{tot} . The set of measured cascade trajectories results in a set of total entropy variation values ΔS_{tot} (the same number of entropy values as the number of trajectories) given by [12,14–16,27]

$$\Delta S_{\text{tot}}[u(\cdot)] = - \int_L^\lambda \partial_r u_r \partial_{u_r} \varphi(u_r) dr - \ln \left(\frac{p(u_\lambda, \lambda)}{p(u_L, L)} \right). \quad (5)$$

Based on the Fokker-Planck equation (i.e., the function $D^{(1)}$ and $D^{(2)}$), that describes the stochastic evolution of cascade trajectories in scale, the stochastic potential from the instantaneous stationary solution of the estimated Fokker-Planck equation for a fixed scale is expressed by [13]

$$\varphi(u_r) = \ln [D^{(2)}(u_r, r)] - \int_{-\infty}^{u_r} \frac{D^{(1)}(w_r, r)}{D^{(2)}(w_r, r)} dw_r. \quad (6)$$

As the determination of the total entropy variation possesses a central role in this paper, we discuss Eq. (5) next with respect to its thermodynamic interpretation as well as with respect to the

technical determination. The thermodynamic interpretation is based on the basic relation between heat, work, and inner energy (for further details, see Refs. [15,16,27]). The first term of Eq. (5) is the change in entropy due to the exchange of energy with the surrounding medium, which depends on the evolution through the hierarchy of length scales r in the cascade process. The second term in Eq. (5) is the change in entropy associated with the change in state of the system for a single realization of a process that takes some initial probability $p(u_L, L)$ and changes to a different final probability $p(u_\lambda, \lambda)$.

In Eq. (5), the numerical differentiation of $\partial_r u_r$ is approximated by the central difference quotient, $\lim_{r' \rightarrow r} \frac{u_{r'} - u_r}{r' - r}$. This numerical differentiation is performed for every individual extracted cascade trajectory $[u(\cdot)]$ [see Fig. 1(b)] in a sequence from large to small scales. The derivative of the stochastic potential is performed with respect to the increment u_r ,

$$\partial_{u_r} \varphi(u_r) = \frac{\partial_{u_r} D^{(2)}(u_r, r) - D^{(1)}(u_r, r)}{D^{(2)}(u_r, r)}. \quad (7)$$

The integration in scale is approximated by using rectangles and a midpoint rule discretization of the scale intervals, therefore the integral takes the average of the beginning and end of the discretization interval. The probabilities of starting and ending of the cascade trajectories, u_L and u_λ , can be estimated from the given data. The results shown in the next section depend slightly on the discretization rules and convention. However, the overall statements do not depend on it.

IV. RESULTS

To verify the validity of the estimated $D^{(1,2)}$ describing the cascade process of the turbulent flow correctly, we use the parametrization of $D^{(1,2)}$ [defined in Eqs. (3) and (4)] to reconstruct structure functions $S^k(r) = \langle u_r^k \rangle$ of order k (see Refs. [10,24,28,29]). Our results show an accurate agreement between measurements and reconstructed data, as shown in Fig. 2(c) for the scalewise evolution of third- and sixth-order structure functions. This reconstruction also includes the experimentally found deviations from scaling behavior by Kolmogorov [30,31].

As shown above for each cascade trajectory, one obtains a corresponding value of total entropy variation. The set of measured cascade trajectories results in a set of ΔS_{tot} values from which both the integral fluctuation theorem (IFT) and the detailed fluctuation theorem can be tested. The IFT, a fundamental entropy law for nonequilibrium systems [16,27], expresses the integral balance between the entropy-consuming ($\Delta S_{\text{tot}} < 0$) and the entropy-producing ($\Delta S_{\text{tot}} > 0$) cascade trajectories. In particular, the IFT holds for any Markovian process, and hence those described by a Fokker-Planck equation [27] and states

$$\langle e^{-\Delta S_{\text{tot}}} \rangle_{[u(\cdot)]} = \int e^{-\Delta S_{\text{tot}}} p(\Delta S_{\text{tot}}) d\Delta S_{\text{tot}} = 1. \quad (8)$$

$\langle \dots \rangle$ is the average over many cascade trajectories and $p(\Delta S_{\text{tot}})$ is the probability density function of the total entropy variation, plotted in Fig. 3(a). This figure shows that the cascade process is linked to an overall entropy production, $\langle \Delta S_{\text{tot}} \rangle > 0$, which is in accordance with the statistical formulation of the second law of thermodynamics. In Fig. 3(b) the convergence of the empirical average is plotted for increasing number N of cascade trajectories. The validity of IFT is fulfilled with a remarkable accuracy better than 10^{-2} (see also Ref. [29]). The fast convergence of the integral fluctuation theorem to the theoretical value, one, together with a good agreement between measured and reconstructed structure functions, are strong indications for the validity of the estimated $D^{(1,2)}$ through our method and therefore the validity of the Fokker-Planck equation for describing the turbulent cascade process.

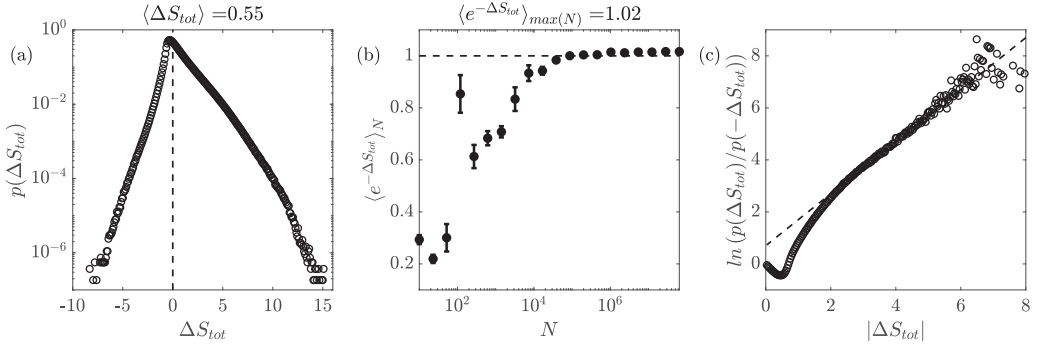


FIG. 3. (a) Probability density function of the total entropy variation S_{tot} . (b) Empirical average $\langle e^{-\Delta S_{tot}} \rangle_N$ of ΔS_{tot} as a function of the number N (sample size) of cascade trajectories $[u(\cdot)]$. According to the integral fluctuation theorem [defined in Eq. (8)], the empirical average has to converge to the horizontal dashed line. (c) Experimental test of the detailed fluctuation theorem [defined in Eq. (9)]. The dashed line in (c) represents a linear fit by using $f(|\Delta S_{tot}|) = |\Delta S_{tot}| + 0.7$.

The detailed fluctuation theorem is a “stronger” theorem which implies the IFT [27]. It is expressed by

$$\ln \left(\frac{p(\Delta S_{tot})}{p(-\Delta S_{tot})} \right) \propto \Delta S_{tot}, \quad (9)$$

$$p(\Delta S_{tot}) \propto p(-\Delta S_{tot})e^{\Delta S_{tot}}. \quad (10)$$

The detailed fluctuation theorem tells us more than the second law of thermodynamics as it supplies a probabilistic character to it: An explicit exponential symmetry constrains one half of the probability distribution which means that even moments can be expressed by the odd ones and vice versa. That symmetry when written in terms of the generating function of $p(\Delta S_{tot})$ reads $\mathcal{G}_{\Delta S_{tot}}(1-x) = \mathcal{G}_{\Delta S_{tot}}(x)$, where x is the conjugate variable of the entropy. Consequently, if the detailed fluctuation theorem is fulfilled, then the probability of entropy-consuming trajectories, which are rare events [as shown in Fig. 3(a)], differs from the probability of frequent entropy-producing trajectories by an exponential factor. Figure 3(c) indicates that for $2 < |\Delta S_{tot}| < 6$ the quantity $\ln [p(\Delta S_{tot})/p(-\Delta S_{tot})] + C$ with a constant value C follows a linear behavior. Thus in addition to the fulfillment of the IFT, the likelihood of occurrence of these rare events is also balanced by a detailed-like fluctuation theorem. If Eq. (9) follows a nonlinear function $g(\Delta S_{tot})$, one speaks of an extended fluctuation theorem (see Ref. [32]).

Next, we ask for typical realizations of turbulent cascade processes. Thus we take cascade trajectories conditioned on a specific total entropy variation and determine for these trajectories the average of the absolute values of the velocity increment $\langle |u_r| \rangle_{\Delta S_{tot}}$ as a function of r (see Fig. 4). As a result of the cascade process through a hierarchy of spatial scales, such defined cascade paths connect the uncorrelated large scale velocity increments $|u_L|$ with the intermittent small scale increments $|u_\lambda|$. Figures 4(a) and 4(b) show that the total entropy variation selects distinct cascade trajectories. Trajectories defined in this way can be divided into two groups. Trajectories marked by entropy production smoothly decrease with a reduction of the length scale, as it is commonly expected for increments. In contrast to this, entropy-consuming trajectories are characterized by a piling up at small scales and a comparable smooth region at large scales.

In Fig. 4(c) we investigate the total entropy dependency of the small scale increments at the end of the cascade process $\langle |u_\lambda| \rangle_{\Delta S_{tot}}$. Note, for an entropy consumption of $\Delta S_{tot} < -2$, a linear increase is found: The larger the total entropy consumption, the larger is the averaged absolute velocity increment at the Taylor length scale. Moreover, Fig. 4(c) indicates that the total entropy consumption is connected to a divergence of absolute velocity increments on the smallest scales

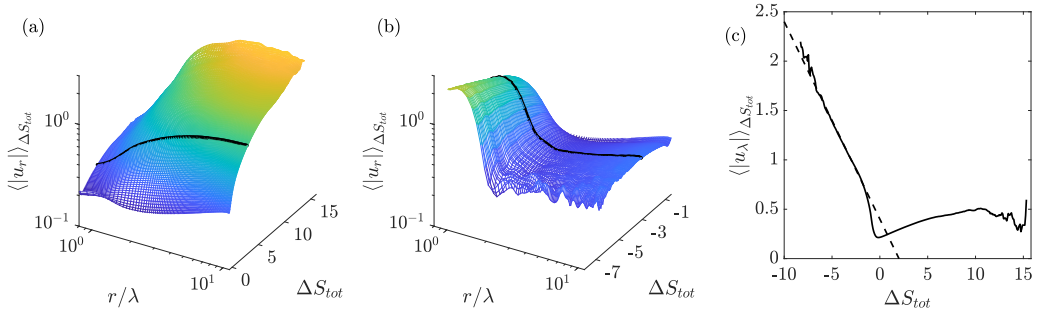


FIG. 4. Mean realization of a turbulent cascade process for (a) positive and (b) negative measured total entropy variation. Solid lines emphasize the averaged absolute velocity increment cascade trajectory for (a) $\Delta S_{tot} = 3$, (b) $\Delta S_{tot} = -3$. (c) Averaged absolute velocity increment at a Taylor length scale conditioned on a specific total entropy variation. The dashed line in (c) represents a linear fit by using $f(|\Delta S_{tot}|) = -0.2\Delta S_{tot} + 0.4$.

since no upper bound in the linear increase for the negative entropy values become obvious [see the dashed line in Fig. 4(c)].

In Figs. 5(a) and 5(b), 200 individual entropy-producing respectively entropy-consuming trajectories, that were used for averaging, are shown. It can be clearly seen that the condition on entropy values selects trajectories of the cascade process with distinctive forms. In order to illustrate that this selection by the total entropy variation is not trivial, we plot in Fig. 5(c) the absolute velocity increment cascade trajectories conditioned on a selected small scale increment value of $|u_\lambda| = 1.5$, i.e., without any entropy condition. Compared to Figs. 4(a), 4(b) and Figs. 5(a), 5(b), no distinct scale behavior on absolute velocity increment cascade trajectories is recognizable.

Further details of the dependency of the velocity increments on the entropy are shown in Fig. 6, where in Fig. 6(a) all initial, large scale increments $|u_L|$ as well as in Fig. 6(b) all final, small scale increments $|u_\lambda|$ are sorted by the total entropy values of the connecting trajectories (see the gray dots). For entropy production all sizes of small and large scale increments are found. Most interestingly, we see that with increasing entropy consumption, a lower bound of small scale increment values becomes obvious [see Fig. 6(b)]. A value zero of small scale increments ($|u_\lambda| \approx 0$) seem to be forbidden.

The mean of the absolute values of the increments conditioned on the total entropy values is shown for small and large scales as black curves in Figs. 6(a) and 6(b). Interestingly, mean large scale increments $\langle |u_L| \rangle_{\Delta S_{tot}}$ depend linearly on the entropy-production values, whereas small

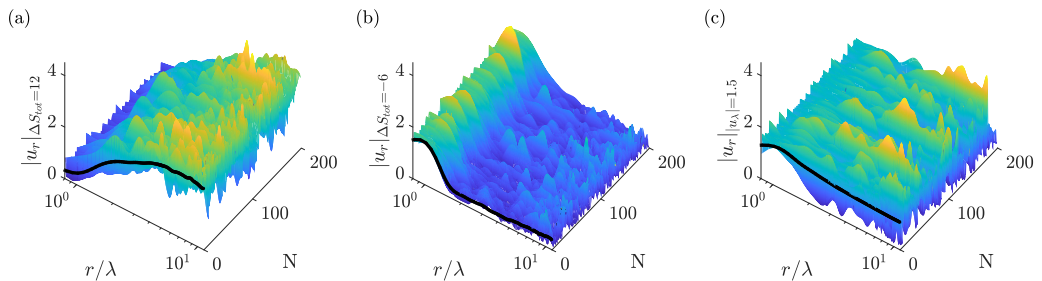


FIG. 5. (a) The first 200 absolute velocity increment cascade trajectories conditioned on a specific total entropy variation (a) $\Delta S_{tot} = 12$, (b) $\Delta S_{tot} = -6$, and (c) conditioned on an absolute velocity increment at a Taylor length scale $|u_\lambda| = 1.5$. Solid lines emphasize the averaged absolute velocity increment cascade trajectory.

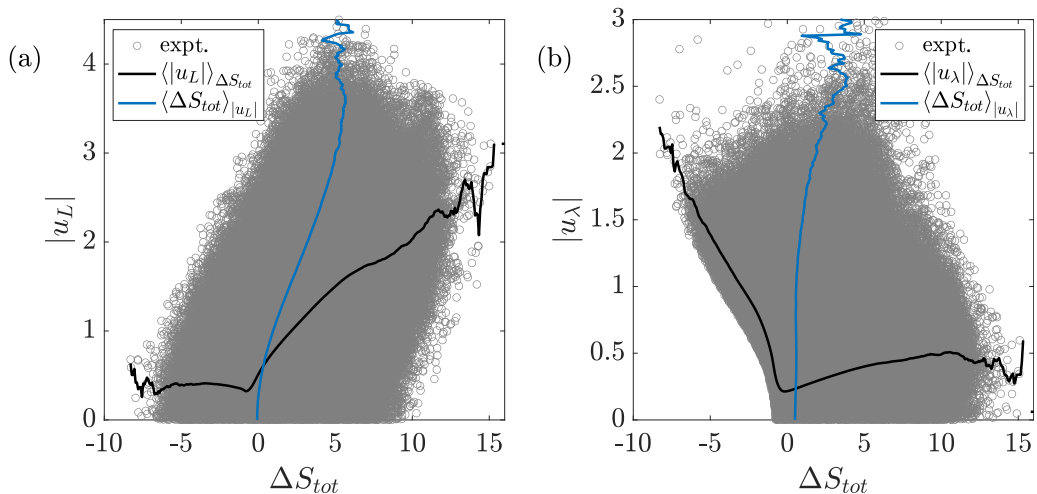


FIG. 6. Scatter plot of velocity increments at (a) large $|u_L|$ and (b) small scales $|u_\lambda|$ as a function of the entropy values of the corresponding cascade trajectory. Black curves represent the mean absolute values of the velocity increments conditioned on the total entropy ΔS_{tot} ; blue curves represent the mean total entropies conditioned on the increment values.

scale increments $\langle |u_\lambda| \rangle_{\Delta S_{tot}}$ show a linear dependency on entropy consumption in a somehow complementary way. From the other parts of the black curves, we see that small scale increments are approximately independent on positive entropy values and that large scale increments are approximately independent on negative entropy values.

The dependencies of the mean total entropies on the velocity increments $\langle \Delta S_{tot} \rangle_{|u_\lambda|}$ are shown as blue curves in Figs. 6(a) and 6(b). Overall for this condition only entropy production is obtained. With an increasing magnitude of the velocity increments (on large as well as on small scales) the entropy indicates the tendency to increase. For zero magnitude of the velocity increments, the entropy is also close to zero, indicating a trivial or equilibrium case.

These two cases of velocity increments conditioned on total entropy variation and entropy conditioned on increments clearly show that the entropy selects interesting information, especially about small scale intermittent structures, on the turbulent velocity field.

V. CONCLUSION

In summary, based on the description of the turbulent cascade process by stochastic equations, a definition for the total entropy variation of each cascade trajectory could be set up. These entropy values follow a rigorous law of nonequilibrium stochastic thermodynamics, namely, the integral fluctuation theorem. Furthermore, large positive and negative entropy events are balanced by the detailed-like fluctuation theorem. Our study shows that these fluctuation relations are highly sensitive to the Kramers-Moyal coefficients $D^{(k)}$. This has largely to do with the fact that minor fluctuations in the coefficients impact the probability distribution, particularly the probability of those unlikely entropy-consuming events which are crucial to obtaining the relations.

These fundamental statistical fluctuation theorems are linked to distinct cascade trajectories in such a way that the total entropy variation allows defining mean trajectories leading to different interesting small scale structures. For positive entropy values velocity increments have the tendency to decay with decreasing scale, as it fits well to the traditional picture of turbulence. For negative entropy values an anomalous behavior is found, namely, the conditioned trajectories show building up increments for decreasing scale leading to jumps or quasisingularities on small scales, similarly to what is observed in Ref. [5]. Taking the large increments of entropy-consuming trajectories

as quasisingularities and the entropy-producing trajectories as classical nonsingular behavior, the detailed-like fluctuation theorem sets the occurrence of entropy-producing in direct relation with entropy-consuming trajectories. The exponential proportionality factor between both entropies may be taken as the depletion law for the quasisingular behavior in the sense that more singular cascade trajectories have a higher amount of traditional entropy-producing trajectories as a counterpart (see the analogy to the occurrence of rogue ocean waves [33]).

The results on the selection of distinct cascade trajectories by the total entropy variation and the distribution $p(\Delta S_{\text{tot}})$ indicate that no saturation tendency becomes obvious for minimal and maximal total entropy variation, thus for the corresponding piling up velocity differences of the small scale structures. Furthermore, the negative entropy effect goes along with the appearance of a lower bound for small scale increments. This finding might be of interest to the questions of singularities or rare extreme velocity gradients at small scales (see Ref. [7]). We leave the implications of these observations open for further study.

In our opinion, this interdisciplinary treatment of the turbulent cascade process has the potential to be an alternative way to link the statistical description of turbulence (via common two-point increment statistics), nonequilibrium stochastic thermodynamics, and local turbulent flow structures.

ACKNOWLEDGMENTS

We acknowledge helpful discussions with A. Abdulrazek, J. Friedrich, J. Ehrich, A. Engel, G. Gülker, S. Kharche, D. Nickelsen, and T. Wester. We acknowledge financial support by DFG (PE 478/18-1, WA 3793/2-1, LI 1599/3-1), FAPERJ (Jovem Cientista do nosso Estado 202.881/2015), CNPq (306477/2016-5), and from the Laboratoire d'Excellence LANEF in Grenoble (ANR-10-LABX-51-01).

-
- [1] S. B. Pope, *Turbulent Flows* (Cambridge University Press, Cambridge, UK, 2001).
 - [2] U. Frisch, *Turbulence, the Legacy of A. N. Kolmogorov* (Cambridge University Press, Cambridge, UK, 1995).
 - [3] P. Davidson, *Turbulence: An Introduction for Scientists and Engineers* (Oxford University Press, Oxford, UK, 2015).
 - [4] C. L. Fefferman, Existence and smoothness of the Navier-Stokes equation, *Millenn. Prize Probl.* **57**, 67 (2006).
 - [5] P. Debue, V. Shukla, D. Kuzzay, D. Faranda, E.-W. Saw, F. Daviaud, and B. Dubrulle, Dissipation, intermittency, and singularities in incompressible turbulent flows, *Phys. Rev. E* **97**, 053101 (2018).
 - [6] T. Grafke, R. Grauer, and T. Schäfer, Instanton filtering for the stochastic Burgers equation, *J. Phys. A* **46**, 062002 (2013).
 - [7] D. Buaria, A. Pumir, E. Bodenschatz, and P.-K. Yeung, Extreme velocity gradients in turbulent flows, *New J. Phys.* **21**, 043004 (2019).
 - [8] D. Kleinhans, R. Friedrich, A. Nawroth, and J. Peinke, An iterative procedure for the estimation of drift and diffusion coefficients of Langevin processes, *Phys. Lett. A* **346**, 42 (2005).
 - [9] R. Friedrich and J. Peinke, Description of a Turbulent Cascade by a Fokker-Planck Equation, *Phys. Rev. Lett.* **78**, 863 (1997).
 - [10] A. P. Nawroth, J. Peinke, D. Kleinhans, and R. Friedrich, Improved estimation of Fokker-Planck equations through optimization, *Phys. Rev. E* **76**, 056102 (2007).
 - [11] C. Renner, J. Peinke, R. Friedrich, O. Chanal, and B. Chabaud, Universality of Small Scale Turbulence, *Phys. Rev. Lett.* **89**, 124502 (2002).
 - [12] N. Reinke, A. Fuchs, D. Nickelsen, and J. Peinke, On universal features of the turbulent cascade in terms of non-equilibrium thermodynamics, *J. Fluid Mech.* **848**, 117 (2018).
 - [13] J. Peinke, M. R. R. Tabar, and M. Wächter, The Fokker-Planck approach to complex spatiotemporal disordered systems, *Annu. Rev. Condens. Matter Phys.* **10**, 107 (2019).

- [14] D. Nickelsen and A. Engel, Probing Small-Scale Intermittency with a Fluctuation Theorem, *Phys. Rev. Lett.* **110**, 214501 (2013).
- [15] K. Sekimoto, *Stochastic Energetics* (Springer, Berlin, 2010), Vol. 799.
- [16] U. Seifert, Entropy Production Along a Stochastic Trajectory and an Integral Fluctuation Theorem, *Phys. Rev. Lett.* **95**, 040602 (2005).
- [17] D. J. Evans, E. G. D. Cohen, and G. P. Morriss, Probability of Second Law Violations in Shearing Steady Flows, *Phys. Rev. Lett.* **71**, 2401 (1993).
- [18] G. Gallavotti and E. G. D. Cohen, Dynamical Ensembles in Nonequilibrium Statistical Mechanics, *Phys. Rev. Lett.* **74**, 2694 (1995).
- [19] J. Kurchan, Fluctuation theorem for stochastic dynamics, *J. Phys. A* **31**, 3719 (1998).
- [20] D. Collin, F. Ritort, C. Jarzynski, S. Smith, I. Tinoco, Jr., and C. Bustamante, Verification of the Crooks fluctuation theorem and recovery of RNA folding free energies, *Nature (London)* **437**, 231 (2005).
- [21] J. Gomez-Solano, C. July, J. Mehl, and C. Bechinger, Non-equilibrium work distribution for interacting colloidal particles under friction, *New J. Phys.* **15**, 045026 (2015).
- [22] N. Mazellier and J. Vassilicos, Turbulence without Richardson-Kolmogorov cascade, *Phys. Fluids* **22**, 075101 (2010).
- [23] G. I. Taylor, The spectrum of turbulence, *Proc. R. Soc. A* **164**, 476 (1938).
- [24] C. Renner, J. Peinke, and R. Friedrich, Experimental indications for Markov properties of small-scale turbulence, *J. Fluid Mech.* **433**, 383 (2001).
- [25] S. Lueck, C. Renner, J. Peinke, and R. Friedrich, The Markov-Einstein coherence length—A new meaning for the Taylor length in turbulence, *Phys. Lett. A* **359**, 335 (2006).
- [26] H. Risken, *The Fokker-Planck Equation* (Springer, Berlin, 1989).
- [27] U. Seifert, Stochastic thermodynamics, fluctuation theorems and molecular machines, *Rep. Prog. Phys.* **75**, 126001 (2012).
- [28] R. Stresing and J. Peinke, Towards a stochastic multi-point description of turbulence, *New J. Phys.* **12**, 103046 (2010).
- [29] M. Gorokhovski and F. S. Godefert, *Turbulent Cascades II—Proceedings of the Euromech-ERCOFTAC Colloquium 589* (Springer, Cham, 2019).
- [30] A. N. Kolmogorov, Dissipation of energy in locally isotropic turbulence, *Dokl. Akad. Nauk SSSR* **32**, 16 (1941).
- [31] A. N. Kolmogorov, A refinement of previous hypotheses concerning the local structure of turbulence in a viscous incompressible fluid at high Reynolds number, *J. Fluid Mech.* **13**, 82 (1962).
- [32] H. Touchette, The large deviation approach to statistical mechanics, *Phys. Rep.* **478**, 1 (2009).
- [33] A. Hadjihoseini, P. G. Lind, N. Mori, N. P. Hoffmann, and J. Peinke, Rogue waves and entropy consumption, *Europhys. Lett.* **120**, 30008 (2018).